AD-A174 436 SATURATION AND SPECTRAL LINE BEHAVIOR IN THE RESONANT CARS SPECTRUM OF OH (U) UNITED TECHNOLOGIES RESEARCH CENTER EAST HARTFORD CT J F VERDIECK ET AL 30 MAY 86 1/1

UNCLASSIFIED UTRC/R86-957058F AFOSR-TR-86-1087 F/G 7/4 NL

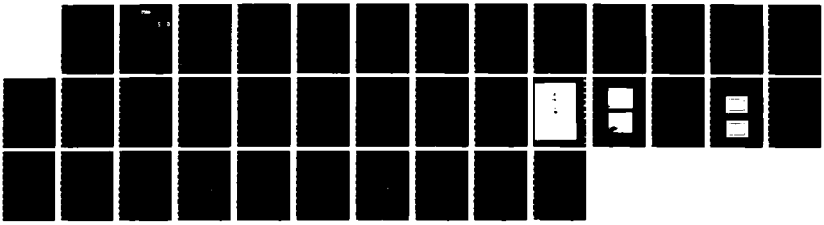

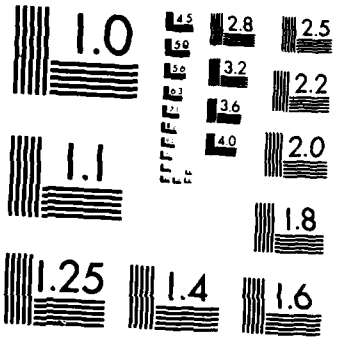

MICROCOPY RESOLUTION TEST CHART
NATIONAL BUREAU OF STANDARDS-1963-A

AD-A174 436

AFOSR-TR- 86-1087

UNITED TECHNOLOGIES RESEARCH CENTER

East Hartford, Connecticut 06108

DTIC ELECTE NOV 26 1986 S D

F49620-85-C-0014

Saturation and Spectral Line Behavior in the Resonant CARS Spectrum of OH

Approved for public release; distribution unlimited.

DTIC FILE COPY

DATE May 1986

86 11 26 064

UNCLASSIFIED

SECURITY CLASSIFICATION OF THIS PAGE

REPORT DOCUMENTATION PAGE

1a. REPORT SECURITY CLASSIFICATION UNCLASSIFIED	1b. RESTRICTIVE MARKINGS
2a. SECURITY CLASSIFICATION AUTHORITY	3. DISTRIBUTION/AVAILABILITY OF REPORT Approved for public release, distribution unlimited
2b. DECLASSIFICATION/DOWNGRADING SCHEDULE	
4. PERFORMING ORGANIZATION REPORT NUMBER(S) R86-957058F	5. MONITORING ORGANIZATION REPORT NUMBER(S) AFOSR-TR- 86-1087
6a. NAME OF PERFORMING ORGANIZATION United Technologies Research Center 6b. OFFICE SYMBOL (If applicable)	7a. NAME OF MONITORING ORGANIZATION Air Force Office of Scientific Research/NA
6c. ADDRESS (City, State and ZIP Code) Silver Lane East Hartford, CT 06108	7b. ADDRESS (City, State and ZIP Code) Bolling AFB DC 20332-6448
8a. NAME OF FUNDING/SPONSORING ORGANIZATION Air Force Office of Sci. 8b. OFFICE SYMBOL (If applicable) AFOSR/NA	9. PROCUREMENT INSTRUMENT IDENTIFICATION NUMBER F49620-85-C0014
8c. ADDRESS (City, State and ZIP Code) Bolling AFB D.C. 20332	10. SOURCE OF FUNDING NOS. PROGRAM ELEMENT NO.: 61102F PROJECT NO.: 2308 TASK NO.: A3 WORK UNIT NO.:
11. TITLE (Include Security Classification) UNCLASSIFIED Saturation and Spectral Line Behavior in the Resonant CARS of OH	
12. PERSONAL AUTHOR(S) J. F. Verdieck, L. R. Boedeker	
13a. TYPE OF REPORT Final Scientific 13b. TIME COVERED FROM 12/1/84 TO 4/30/86	14. DATE OF REPORT (Yr., Mo., Day) 86,5,30 15. PAGE COUNT 32
16. SUPPLEMENTARY NOTATION	

17. COSATI CODES			18. SUBJECT TERMS (Continue on reverse if necessary and identify by block number)
FIELD	GROUP	SUB. GR.	Combustion Diagnostics,
21	02		CARS, Resonant Enhancement
20	13		Hydroxyl Radical, Saturation

19. ABSTRACT (Continue on reverse if necessary and identify by block number)

This contract has explored the origins of the unpredicted satellite lines about the central resonance of the CARS spectrum found in a previous study. The objectives of the program were to determine the dependence of the line structure on the input laser intensities and on tuning of the resonant frequency. Data from these experiments would then suggest a choice of mechanism responsible for the satellite structure. In the previous AFOSR-supported study, electronically resonant coherent anti-Stokes Raman spectroscopy (CARS) of OH was demonstrated for the first time using a flame source. Theory and experiment were in generally good agreement, except for the presence of satellite lines ("extra resonances") about the strong central component.

In order to investigate reliably the power dependence of the resonance CARS spectrum and thereby test for saturation effects, a single mode, pulsed, tunable dye laser was

20. DISTRIBUTION/AVAILABILITY OF ABSTRACT UNCLASSIFIED/UNLIMITED ☑ SAME AS RPT. ☐ DTIC USERS ☐	21. ABSTRACT SECURITY CLASSIFICATION Unclassified
22a. NAME OF RESPONSIBLE INDIVIDUAL Julian M. Tishkoff	22b. TELEPHONE NUMBER (Include Area Code) (202) 767-4935 22c. OFFICE SYMBOL AFOSR/NA

DD FORM 1473, 83 APR EDITION OF 1 JAN 73 IS OBSOLETE.

UNCLASSIFIED

SECURITY CLASSIFICATION OF THIS PAGE

utilized to insure selective excitation of a single resonance. The resultant spectra show clearly that saturation occurs at input laser pulse energies of the resonant frequency of about 0.1 millijoules. Under our operating conditions, 5 nsec pulse width, 0.01 cm focal spot, this corresponds to an intensity of approximately 2×10^8 W/cm^2. Saturation effects are particularly apparent when the CARS pump frequency is on line center of the selected electronic transition. Tuning away from line center and/or reducing input pulse energy produces a notable decrease in the strength of the satellite lines relative to the central peak. The central peak, in turn, increased relative to the adjacent water CARS spectrum and appeared to have a simplified spectrum. The frequency splitting between the satellite components was determined to be independent of laser intensity and the tuning of the resonant CARS pump frequency relative to line center. Indeed, the observed splittings are constant among all spectral recorded, regardless of experimental conditions. These observations imply that the observed satellite splittings do not correspond to a field-dependent Rabi frequency splitting. Nor is a PIER-4 type of phenomenon a likely cause because the observed satellite splittings did not depend upon tuning of the CARS resonant frequency. The most reasonable explanation is that the satellite lines have their origin from a redistribution in population of rotational energy levels in the upper electronic state during the laser pulse. Such energy transfer, driven by the saturation of the electronic transition, is known from saturated fluorescence studies of diatomic molecules. This last explanation, while reasonable, remains to be proven by further experiments and computer calculations.

R86-957058F

Saturation and Spectral Line Behavior in the Resonant CARS Spectrum of OH

TABLE OF CONTENTS

	PAGE
ABSTRACT	1
INTRODUCTION	2
EXPERIMENTAL	5
RESULTS AND DISCUSSION	8
CONCLUSIONS	12
SUGGESTIONS FOR FURTHER WORK	13
REFERENCES	13
ACKNOWLEDGEMENTS	14
FIGURES	15

COPY INSPECTED

Accesion For
NTIS CRA&I ☑
DTIC TAB ☐
Unannounced ☐
Justification
By
Distribution /
Availability Codes
Dist | Avail and / or Special
A-1

Saturation and Spectral Line Behavior in the Resonant CARS Spectrum of OH

James F. Verdieck and Laurence R. Boedeker

Abstract have been explored

This contract has explored the origins of the unpredicted satellite lines about the central resonance of the CARS spectrum found in a previous study. The objectives of the program were to determine the dependence of the line structure on the input laser intensities and on tuning of the resonant frequency. Data from these experiments would then suggest a choice of mechanism responsible for the satellite structure. In the previous AFOSR-supported study, electronically resonant coherent anti-Stokes Raman spectroscopy (CARS) of OH was demonstrated for the first time using a flame source. Theory and experiment were in generally good agreement, except for the presence of satellite lines ("extra resonances") about the strong central component.

In order to investigate reliably the power dependence of the resonance CARS spectrum and thereby test for saturation effects, a single mode, pulsed, tunable dye laser was utilized to insure selective excitation of a single resonance. The resultant spectra show clearly that saturation occurs at input laser pulse energies of the resonant frequency of about 0.1 millijoules. Under our operating conditions, 5 nsec pulse width, 0.01 cm focal spot, this corresponds to an intensity of approximately 2×10^8 W/cm^2. Saturation effects are particularly apparent when the CARS pump frequency is on line center of the selected electronic transition. Tuning away from line center and/or reducing input pulse energy produces a notable decrease in the strength of the satellite lines relative to the central peak. The central peak, in turn, increased relative to the adjacent water CARS spectrum and appeared to have a simplified spectrum. The frequency splitting between the satellite components was determined to be independent of laser intensity and the tuning of the resonant CARS pump frequency relative to line center. Indeed, the observed splittings are constant among all spectra recorded, regardless of experimental conditions. These observations imply that the observed satellite splittings do not correspond to a field-dependent Rabi frequency splitting. Nor is a PIER-4 type of phenomenon a likely cause because the observed satellite splittings did not depend upon tuning of the CARS resonant frequency. The most reasonable explanation is that the satellite lines have their origin from a redistribution in population of rotational energy levels in the upper electronic state during the laser pulse. Such energy transfer, driven by the saturation of the electronic transition, is known from saturated fluorescence studies of diatomic molecules. This last explanation, while reasonable, remains to be proven by further experiments and computer calculations.

Introduction

Under a previous AROSR Contract, the electronically resonant CARS (coherent anti-Stokes Raman spectroscopy) spectrum of the OH radical was observed for the first time.[1] The hydroxyl radical was chosen for study at this laboratory because of its ubiquitous presence and extreme importance in combustion chemistry. OH enters into the oxidation mechanisms of nearly all hydrogen-containing fuels, expecially hydrocarbons. Hydroxyl radical reactions are usually very rapid (because OH is a radical, activation energies are small) and often rate-determining in combustion mechanisms. OH is also important in atmospheric chemistry and in particular, is implicated in acid rain formation by reaction with nitrogen and sulfur oxides. For these important reasons, it is important to be able to detect and measure the concentration of the OH radical in environments difficult to probe with conventional means.

At the present time, the diagnostic method of choice for species of low concentration is laser-induced fluorescence (LIF). LIF is a point measurement technique which enjoys good success in carefully controlled laboratory devices operating cleanly at low pressure (one atmosphere or less). However, in practical combustion environments, fluorescence methods can suffer from interferences, such as fluorescence from other species, and from laser-induced particle incandescence. The other major disadvantage with fluorescence techniques is collisional quenching, which may prove to be particularly severe for application in high pressure devices. For this particular application, resonant CARS may be the superior technique. The principal reason for the success of CARS methods in these difficult combustion systems is the fact that the CARS signal emerges as a coherent beam, all of which can be captured by the optical detector. This provides a unique advantage over incoherent techniques, such as fluorescence, particularly when the optical access is limited and small f-number optics cannot be employed. Because CARS methods have proven superior for these cases, it is essential to extend the sensitivity of CARS to radicals such as OH and other minority species. Electronically resonant CARS, because of the intrinsic orders of magnitude enhancement in signal strength, is the technique of choice.

Resonant CARS was achieved for several different electronic transitions in the A --> X band of OH in a methane/oxygen flame. Concurrently with the experimental studies, a good understanding of the theoretical aspects of the resonant CARS process was secured. Predicted resonant CARS spectra could be computer synthesized and graphed for any selected resonance excitation, which agreed well with experimental spectra with regard to the major features. However, saturation effects were not considered in the theoretical treatment.

A major departure from theoretical predictions was the experimental observation of satellite lines about the central line. It was suspected that the major cause of the discrepancy between theory and experiment was that the experimental beam energies corresponded to conditions of saturation. Preliminary tests for saturation were performed and definite evidence was found, both in the intensity variation in the spectrum, and the number and shape of the lines observed. In order to realize the full potential of resonant CARS as a useful diagnostic technique, it was felt mandatory to address the fundamental physics underlying the appearance of the unpredicted satellites in the resonant CARS spectrum. The limiting detectivity of resonant CARS may in fact depend upon whether or not the experiment is carried out under saturation conditions. Moreover, the quantitative application may require an explanation of saturation effects, although a working curve of concentration vs signal strength may be prepared if a suitable means of calibration can be found.

There are several possible causes for the appearance of satellite lines ("extra resonances") in resonant CARS; these are: saturation, dephasing effects brought about by pressure and/or other factors, and rotational energy transfer redistribution of states. Each of these is discussed briefly in turn.

Saturation of the ordinary CARS effect occurs when the optical field strengths of the incident laser beams cause significant population of the upper Raman state. For the case of resonance CARS, a further complication arises, namely, the upper (resonant) electronic state can be significantly populated by the ω_1 laser beam. This latter phenomenon, which is also observed and exploited in saturated laser-induced fluorescence diagnostic methods, occurs readily because of the strongly allowed transition to this state. The significant population in the upper states implies that the mathematical treatment of the CARS interaction can no longer be treated by perturbation theory, at least to low order. For this reason, most previous theoretical treatments of resonant CARS do not include saturation. However, there have appeared non-perturbative approaches to the strong-field case. One of the most interesting results of these treatments of saturation comes from the work of Wilson-Gordon, Klimovsky-Baird, and Friedmann.[2] These authors predict that, for the case of both the ω_1 and ω_2 fields strong, the resonant CARS spectrum will be split, by Stark splitting, into five components. The magnitude of the splitting is proportional to the so-called Rabi frequency, whose value is given by the product of the transition dipole moment and the electric field strength. Dick and Hochstrasser[3] also predict Stark splitting of the resonant CARS spectrum. Their prediction of a doublet splitting is in agreement with Wilson-Gordon, et al., for the case of only one strong field. The salient feature of both treatments is that the splitting of the extra components in the resonant spectrum is dependent upon the laser intensity.

Another explanation for the appearance of the satellite structure is the so called PIER-4 (pressure induced extra resonances in 4-wave mixing) effect observed in sodium vapor by Prior, Bodgan, Dagenais, and Bloembergen.[4] Similar effects have been observed by Hochstrasser and coworkers, and have been termed DICE (dephasing-induced coherent emission) effects.[5] These effects derive from a term in the differences between linewidths for the transitions involved in the wave-mixing process of interest. This dephasing or damping term can result in extra resonances under certain conditions. In the case of Prior et al., the PIER-4 resonance is observed when the ω_1 frequency is tuned 5 cm^{-1} off of resonance. It is distinguished from the resonant CARS signal by it pressure dependence, and apparently, to the tuning of ω_1 off resonance.

Yet a third possibility is rotational energy level population redistribution in the upper electronic state, A, occurring during the period of the laser pulse. This process can and does occur as evidenced by the appearance of fluorescent lines adjacent to the resonant fluorescent line in the LIF spectra of diatomic molecules.[6] In the upper electronic state, energy transfer from the resonant rovibronic level to adjacent levels (initially of very small population) is driven by the highly excess population in the resonant level. This leakage from the resonant level to nearby levels, is the major reason why saturation is so difficult to achieve with molecules as compared with atomic systems. The situation just described must be melded in with the CARS process which would lead to the appearance of extra resonances. Preliminary calculations indicate that the additional lines which might arise from rotational population redistribution would be split from the central line by about 30 cm^{-1}; however, these calculations were limited to Q-branch transitions only. A much more thorough calculation, involving all levels and all possible transitions, including partially forbidden ones should be performed.

It was also noted in the previous study that the entire resonant CARS spectrum is a very sensitive function of the tuning of the CARS pump frequency, ω_1. Rather minute changes in the position of the pump frequency rendered profound changes in the number, position, shape and relative intensities of the lines of the resonant CARS spectrum. This was not an original observation. Numerous workers in the field of resonant CARS, particularly those working with large molecules in solution phase have noticed similar effects.[7] Indeed, changes from dispersion to absorption line shapes, and reversal of sign (i.e., negative-going lineshapes relative to the non-resonant background) have been observed from nitrosoaniline in solution as the pump frequency is tuned through the absorption band.[8] It should be noted that, for these cases, the electronic absorption bands can be fifty to a hundred nanometers wide. There appears to have been few, if any, similar

studies of detailed tuning through a narrow line resonance, such as those found for diatomic molecules. The one notable exception is the work of Attal, et al., on resonant CARS of the C_2 molecule.[9] These authors noted that tuning shifts in ω_1 as small as 0.06 cm^{-1} caused dramatic changes in the appearance of the resonant CARS spectrum.

In order to properly assess the effects of tuning through the line center of the resonance excitation, and separate out these effects from those due to saturation, it was mandatory to employ a laser source with a linewidth less than that of the transition under study. A single-mode dye laser, patterned after the design of Littman,[10] was utilized to fulfill this requirement. The construction, operation and performance of this laser system are described in detail in the experimental section.

Experimental

The experimental approach employed in this study of OH electronic resonant CARS is similar to that used previously,[1] and will not be extensively discussed. The most important new features are the incorporation of a single mode dye laser (SMDL) and a Fizeau wavemeter (Lasertechnics) into the resonant CARS apparatus, shown schematically in Fig. 1. The CARS pump beam, ω_1, which excites a selected OH electronic resonance, is obtained by frequency doubling the output from the narrowband, single mode, tunable, pulsed dye laser (SMDL). In the prior study ω_1 originated from a highly multimode, larger bandwidth dye laser. The lack of precise mode definition and bandwidth relative to the OH line profile prevented precise tuning, thereby precluding an understanding of the OH resonant CARS spectral structure observed. The addition of the wavemeter to the resonant CARS system provided rapid and accurate tuning of the CARS pump frequency to the desired resonant transition.

In Fig. 1, SMDL is a narrowband, pulsed dye laser that has been assembled at UTRC, based on the dye oscillator design of Littman.[10] In Littman's approach to the design of a SMDL, an extended length of the grating is illuminated by employing a very small, grazing incidence angle between the laser optical axis and the grating surface, typically 1 degree. In addition the cavity is made very short, about 5 cm, which allows for many photon round trips when a 5-10 ns pump pulse is employed, and also introduces a large axial mode separation, about 2-3 GHz. Littman has measured a bandwidth of about 150 MHz for the single mode output beam. Additionally, the SMDL oscillator is end-pumped, rather than side-pumped; this provides a much better defined mode volume and results in a uniform, circular beam spot. Figure 2 shows in block form the several diagnostic instruments used to measure the important parameters of the SMDL which are necessary to perform the resonant CARS experiments.

A photograph of our Littman single-mode oscillator is shown in Fig. 3, pumped with about 4 mJ of the 532.0 nm Nd:YAG beam. The horizontal U-shaped dye cell, with the focussed spot of the pump beam readily apparent, lies between the circular back mirror and the grating (rectangular square object). The 2.5 cm tuning mirror, on the left, sets the scale for the photograph. The oscillator output beam, with unknown output energy, is amplified to a pulsed energy level of about 10 mJ using a 3-stage amplifier chain. Frequency-doubled 280 nm pulses with energies of about 1 mJ have been obtained. The longitudinal mode structure of the amplified output beam at 560 nm is examined by projecting the Fabry-Perot pattern generated with a solid etalon (0.7 cm^{-1} free spectral range) on a white sheet of paper. Two typical patterns are shown in Fig. 4. Figure 4a shows a pattern in which a single longitudinal mode is clearly evident. By contrast, Fig. 4b indicates the presence of some additional very weak modes. The photos were taken with a one second exposure, and hence represent a 10 laser shot average. Fine adjustment of the mode structure, at a given frequency setting of the tuning mirror, was accomplished using a technique recommended by Littman,[11] in which precise rotation of the dye cell is used to accomplish small changes in the optical path.

Two additional factors are critically important in obtaining stable single-mode operation: temporal smoothness of the 532.0 nm pump pulse into the oscillator,[11] and steadiness of the dye flow through the small oscillator dye cell. The multimode output of the Quanta-Ray Nd:YAG laser at 532.0 nm is smoothed temporally, using a demodulator[12] prior to pumping both dye lasers. Demodulation effects a marked improvement on shot-to-shot stability of the Littman oscillator, and improves the temporal smoothness and repeatability in all amplifier stages. Satisfactory dye flow stability in the oscillator is achieved by using gravity feed from a reservoir 1 meter above the optical table. The precise linewidth of the UTRC SMDL output beam at 560 nm will be the subject of continuing studies using a Burleigh scanning Fabry-Perot interferometer; however, it is estimated from the Fabry-Perot patterns that the linewidth is less than 0.1 cm^{-1}.

A key diagnostic in the present experiment is the precise measurement of both pulsed dye laser frequencies. This is achieved by determining the fundamental frequencies (in the visible) with a Lasertechnics Fizeau wavemeter, accurate to 1 part in 10^6. In this instrument, a large number of fringes are generated by a precision, vacuum gap, small-angle wedge interferometer (Fizeau). The fringes are imaged onto a diode array and counted by means of an on-line microcomputer (IBM PC/XT). The computer calculates the frequency or wavelength from this count and stored constants determined from a previous calibration. The frequency/wavelength calculation and display on the computer terminal are updated at a sample rate of the

operator's choice; between 10 and 17 laser shots was selected here. The addition of the wavemeter capability to the resonant CARS facility has made it possible to locate quickly and precisely the selected OH transition for the present CARS studies $Q_1(4)$, using fluorescence detection. The present experiments used the same burner and CH_4/O_2 flame that had been employed previously.[1]

The $Q_1(4)$ excitation spectrum, as monitored by R-branch fluorescence excited by incrementally tuning the SMDL, is displayed in Fig. 5. Fluorescence was observed in the R-branch instead of the $Q_1(4)$ resonance in order to avoid Rayleigh scattering interference. The fluorescence peak signal level was measured by visual estimate of the photomultiplier (PMT) output pulse on a fast (200 psec), intensified oscilloscope. At any given setting of $\omega_1/2$ the wavemeter indicated that the stability of SMDL was about ±0.02 cm^{-1} over a 5-10 minute period, which is approximately the accuracy limitation of the wavemeter. These data locate the line center at about twice 17,699.4 cm^{-1}. This value is about 0.8 cm^{-1} greater than calculated from the energy levels recently given by Coxon,[13] and almost 2 cm^{-1} more than that given in the classic study of Dieke and Crosswhite.[14] This discrepancy may arise because the wavemeter was not recalibrated near the frequency of the OH resonance. More precise experiments will be required to characterize the linewidth, if saturation effects are to be accounted for. The value derived from Fig. 5 is approximately 0.3 cm^{-1}, which agrees favorably with OH linewidths in flames determined from absorption[15] and from LIF[16] which are about 0.4 cm^{-1}. The excitation scan also indicates the presence of a nearby, weak transition at $\omega_1/2$ = 17,701.2 cm^{-1}, probably $R_2(1)$. While ω_1 was located at linecenter of $Q_1(4)$ the fluorescence spectrometer was scanned, and the appropriate P, Q and R branch signals were confirmed, as in the prior studies[1].

The $Q_1(4)$ transition was chosen for the study of saturation and spectral line behavior because in the previous study this particular transition produced strong resonant CARS spectra relative to the adjacent water CARS spectrum. For the purpose of this study, the generation of electronically resonant CARS spectra of OH was limited to this key transition. Several values of ω_1 relative to the center of the $Q_1(4)$ transition, and different levels of pump and Stokes beam intensities were employed to help unravel the origin of the extra resonances observed in the first study.

The temporal character of ω_1 and ω_2 prior to doubling were investigated with aid of a fast photo-diode and an intensified oscilloscope, having an overall response time of about 0.2 ns. The oscilloscope photographs shown in Fig. 6a indicate that the $\omega_1/2$ yellow beam from the SMDL was about 4-5 ns FWHM. The red beam, $\omega_2/2$ from the Quanta-Ray dye laser (PDL-1) was 6-7 ns FWHM, shown in Fig. 6b. The doubled

beams at ω_1, ω_2 are expected to be temporally narrower. These temporal studies are required to adjust optical path lengths to achieve simultaneous arrival of peak ω_1 and ω_2 intensities in the CARS focal generation zone in the flame. The pump and Stokes beams are focussed by a common lens, and aligned to pass through a small aperture at the focus to achieve maximum beam overlap for CARS generation. These low-power (less than 1 mJ each) uv beams are capable of burning holes in white cards through which about 60 % of the beam energy is subsequently transmitted. The hole produced by the focussed ω_1 beam is typically 100 microns in diameter, while ω_2 produces an oval hole about 100 X 150 microns in size. It is possible to adjust the SMDL to achieve single-mode etalon patterns for a range of pulse widths from about 2 to 6 ns, indicating that more than one cavity length may be operative, depending upon focussing position in the cell and/or pattern on the grating. The shape of the pulse varies from very smooth (perhaps near Gaussian) at 2 ns to fast-rise, flat-topped at 6 ns. The longer, flat-topped pulse may be an indication of quasi-cw operation that is expected from the very short cavity length Littman oscillator. The pulse energies at frequency ω_1 appear to scale with this pulse length.

The alignment of the CARS detection system is optimized by the observation of CARS generated from water vapor over a beaker of boiling water. Subsequently, optimization of the pump and Stokes beams alignment, and the second harmonic conversion, are achieved while observing either the water or OH CARS signal on the boxcar averager. Electronically resonant CARS spectra of OH (and water, for reference) in the methane/oxygen flame are recorded directly from the boxcar output with an XY recorder, or transmitted to a PDP computer. The computer provides on-line, real-time display and storage of acquired data on an 8" floppy disk. Data from these runs are transferred to a VAX 11/750 for smoothing, peak analysis, line identification, and plotting.

The resonant CARS spectra are recorded by holding ω_1 fixed (after hand tuning to a desired value), and scanning the Stokes frequency ω_2, while observing the intensity change in the CARS frequency, ω_3. The photomultiplier voltage was adjusted to make the CARS signal approximately full-scale on the output of the boxcar. Frequency markers are recorded on the spectral scans by means of the expediency of unblocking and blocking the input CARS laser beams.

Results and Discussion

The essential results from the present study on saturation and tuning effects in the resonant CARS of OH are contained in the several spectra obtained. The first group of experiments performed examined the changes in the resonant CARS spectrum as the CARS pump frequency was varied across the

$Q_1(4)$ transition. The second group dealt specifically with the issue of saturation and involved reduction of power in either or both of the CARS input laser beams. All spectra were obtained from a methane-oxygen diffusion flame generated by a surface microburner which was operated under nearly identical conditions for all experiments. Similarly the mechanics of recording the resonant CARS spectra were standardized with respect to speed of scanning the Stokes frequency and to placing frequency markers on the spectra. Intensities are only approximately comparable among the various spectra shown due to small changes in alignment of the CARS beams with tuning, and the manual adjustment of both second harmonic crystals which was required by temperature changes and tuning.

Figure 7 presents the electronically resonant CARS spectrum of OH for the $Q_1(4)$ transition for the 1-0 band of the A --> X system. ω_1 is at line center. The OH spectrum extends from approximately 31820 to 31890 cm^{-1} on the Stokes frequency scale, used here for convenience. The (normal) CARS spectrum of H_2O begins at the pronounced dip at 31740 cm^{-1} and extends into the OH spectrum. The strength of the water CARS spectrum provides a benchmark against which the resonant CARS signal may be gauged. For the case shown in Fig. 7, the H_2O and OH signal strengths are comparable. It is noted that some of the lines of the OH spectrum exhibit partial dispersion (derivative) shape. The baseline decline with increasing frequency is a result of the fall in the dye (Exciton DCM) emission curve for the ω_2 dye laser.

In Fig. 8, the same spectral region is displayed with ω_1 tuned approximately 1 cm^{-1} away from line center, toward the higher frequency. The change in the resonant CARS spectrum from that given is Fig. 7 is quite dramatic, with regard to both the strength of the resonant CARS signal (relative to the H_2O CARS) and to the intensity distribution among the lines. The strongest line is only slightly out of range and is estimated to peak (from an XY recorder scan taken previous to this run) at about 16000 to 17000 counts. Note also that this component is wider than the others and appears to have a dispersive component, on the low frequency side. The ratio of the OH CARS signal to that of water CARS is approximately 3 or more. Figure 9 shows a similar spectrum where ω_1 has been tuned further off of line center, more than 2.5 cm^{-1}, and the PMT voltage reduced. For this case the OH resonant CARS spectrum is simpler (fewer lines and a symmetric disposition about the central component) and has an even larger signal relative to the water CARS signal (perhaps 5:1). In Fig. 10 is shown a spectrum taken for ω_1 tuned about 2.5 cm^{-1} to the opposite, low frequency, side of line center of $Q_1(4)$. Note that the PMT voltage is reduced to 1150 volts. The OH/water signal ratio for this case is approximately the same as is Fig. 9; the absolute value for the resonant CARS signal is the largest for any of the spectra presented, if the PMT voltage

changes were taken into consideration. Of particular interest is the strong central line of the spectrum which has a dispersive component (on the high frequency side) that has driven the trace to the lowest limit possible, namely the residual signal pickup from the ω_1 beam which reaches the PMT. It is also noted that a purely dispersive component, at about 31830 cm^{-1} on the Stokes scale, is evident.

In summary of this group of spectra, it is seen that the signal strength and the number, shape, and intensity distribution of components in the OH resonant CARS spectrum are an extremely sensitive function of the tuning through the resonance transition. From the standpoint of combustion diagnostics, the most interesting aspect of these results is that the resonant CARS signals become stronger as ω_1 is tuned away from the line center. This in itself is an indication that saturation is present at the pulse energies employed for these spectra. The next set of spectra, in which the laser pulse energies are reduced, demonstrates quite convincingly that saturation occurs at pulse energy levels above 0.1 millijoule.

The sequence presented in Figs. 11 to 14 represent spectra taken with the ω_2 energy held constant and the ω_1 energy attenuated; except for PMT voltage changes, the other parameters are the same as for the previous spectra. The spectrum shown in Fig. 11 was recorded on line center with the pulse energy attenuated to approximately 0.2 mJ (down from 0.6 mJ, normal operation) The PMT voltage was raised to 1490 to achieve a full scale reading. This spectrum should be compared with that shown in Fig. 7, also for ω_1 on line center, at full power of the SMDL. It is noted first that the spectrum characterized by one strong central component, with smaller satellites. Secondly, the water CARS spectrum is barely discernible. The signal to noise (and background) ratio is quite good when it is recognized that much of the baseline signal comes from pickup from ω_1 and ω_2 laser beams. The magnitude of signal induced by these sources is indicated by the two square wave components following the resonant spectrum; the first is a measure of the CARS (ω_1) pump energy leaking into the PMT, and the second, the Stokes (ω_2) frequency energy. This sequence is repeated for each of the spectra of the Fig. 11 to 14 series.

The spectra shown in Figs. 12 through 14 were all recorded for ω_1 tuned off line center about 2.5 cm^{-1}, but for different pulse energy values. In the sequence given, the ω_1 pulse energies were measured to be 0.2, 0.1 and a value less than 0.1 mJ. Pulse energies in this range are very difficult to measure because the laser energy meter has considerable drift and is also very susceptible to ambient thermal fluctuations (because it is a calorimeter). Figure 12 may be compared to Fig. 10 because they both refer to the same CARS pump frequency. The general appearance of the two spectra is remarkably similar, except for the ratio of the central line intensity to that

of the components. A purely dispersive line is still seen near 31830 cm^{-1}. The water CARS bandhead dip is barely perceptible in Fig. 13, and not seen at all in Fig. 14. As the ω_1 pulse energy is further reduced, the satellite components continue to diminish relative to the central component; four lines are just barely observed above the noise in the last figure, Fig. 14, for the lowest pulse energy in ω_1 employed. It is at this level of input laser intensity that the experimentally observed resonant CARS spectrum of OH appears to match the theoretically predicted spectrum of reference 1. There are at least four satellite lines still present, although difficult to perceive above the noise. A four point smoothing function was used to reduce the high-frequency noise; Fig. 15 illustrates the effect of this process on the data of Fig.A14. Four satellite lines are clearly evident.

It should be pointed out that when the resonant CARS spectrum was obtained for the lowest pulse energy in ω_1 employed, Fig. 14, it was not possible to observe a fluorescence signal. In all fairness, it must also be admitted that the fluorescence detection system was not optimized for best signal collection; however, it does suggest that resonant CARS may be a competitive technique to LIF for detecting OH or other radical species, under certain circumstances.

Careful scrutiny of the several different spectra (excited at different resonant frequencies relative to the line center) suggested that there was little, if any, change in the line spacing between satellites, as the ω_1 frequency was tuned through the resonant transition. A more revealing examination was achieved by expansion of the spectral region about the OH resonant spectrum. The superposition of three such expansions is shown in Fig. 16, with the resonant frequency indicated, on the right side, for each spectrum. The Stokes frequency scale applies to only the bottom spectrum, but is provided for scale. Marker lines have been drawn through the center of each spectral line. The alignment is self-evident and quite striking. It is seen that even the dispersion shape line, located at slightly less than 31830 cm^{-1}, matches in the two upper spectra. The agreement of satellite component lines was not confined to the three spectra presented in Fig. 16, but applied to nearly all of the spectra taken. The rare exceptions were for those spectra exhibiting distorted or severely broadened lines.

The measured splittings for the lines displayed in Fig. 16 are, reading from the high frequency side of the central peak: 7.9, 8.6, 10.0, and 11.8 cm^{-1}; and to the low frequency side: 5.2, 6.6, and 7.1 cm^{-1}. These values do not form an obvious sequence nor do they correspond to spacings in the emission spectrum of OH.

Conclusions

From the alignment of the upper two spectra it is concluded that a displacement of 2 cm^{-1} in ω_1 does not cause a change in line spacing; from the alignment of the bottom spectrum with the other two it is concluded that the satellite line spacing does not depend upon the incident power in the CARS pump beam, at least not for the power levels employed here The observation that the satellite line spacing does not depend upon the laser intensity would appear to rule out the type of high-field treatment discussed by Wilson-Gordan, et al.,[2] and Dick and Hochstrasser.[3] Clearly, a field-dependent Rabi frequency splitting was not observed for the power levels employed in the resonant CARS experiments performed in this study.

The PIER-4 and DICE types of effects would appear to be eliminated also, on the grounds that these effects are dependent upon tuning of the resonant frequency ω_1, and the presence of unpopulated exited states whose energy separation matches the frequency difference of the two input laser beams. The OH resonant CARS spectra exhibit satellite splittings which do not depend upon the tuning ω_1, and therefore the PIER-4 process is not applicable.

The overwhelming constancy of the observed satellite splittings among all the OH resonant CARS spectra determined in this study lead us to the inescapable conclusion that the spacing of the splittings must relate to some constant(s) of the molecule, most likely involving rotational energy spacings. Moreover, it is known from LIF experiments that saturation-induced leakage from the resonant rovibronic level takes place by collision-induced energy transfer, as stated in the introduction. However, the exact mechanism of origin of the satellites is not obvious. More precise measurements of the satellite spacings obtained by means of slower scanning coupled with computer calculations of energy level differences would help to uncover the mechanism. These and other suggestions for further work are listed below.

A conclusion not relating to the question of satellite structure stems from the observation that resonant CARS signals with good signal-to-noise ratio can be obtained for very low pulse energies, less than 0.1 mJ. It bears repeating that fluorescence was not observed at this low energy of the ω_1 laser beam. Therefore, it appears that resonant CARS should be given serious consideration as a combustion diagnostic. As pointed out previously,[1] even in the saturated regime, it may be possible to construct a working curve of concentration vs signal strength.

Suggestions for Further Work

To gain a full understanding of the origin of the satellites, the following additional experiments are suggested:

1. Obtain more precise frequency data on the line spacings by scanning more slowly through the resonant CARS spectrum, while holding the laser power levels and SMDL frequency constant.

2. Compare the results of 1. with calculations of energy level differences from best available sources.

3. Determine how the results of 1. and 2. depend upon the choice of resonant frequency selected.

4. Compare resonant CARS signals with fluorescence signals, under the best possible conditions for both techniques. This experiment would determine the detectivity limit for resonant CARS and serve to calibrate the method.

5. Perform a resonant CARS experiment on OH in a high pressure burner in order to determine if resonant CARS offers a definite advantage over LIF at high pressures.

References

1. Verdieck, J.F., R.J. Hall, and A.C. Eckbreth, "Electronically Resonant CARS Detection of OH", AIAA 18th Thermophysics Conference, Montreal, Canada, Paper AIAA-83-1477 (1983).

2. Wilson-Gordon, A.D., R Klimovsky-Barid, and H. Friedmann, "Saturation Effects in Coherent Anti-Stokes Raman Scattering," Phys. Rev. A., Vol. 24, 1982, pp. 1580-1595.

3. Dick, B., and R.M. Hochstrasser, "Resonant Non-linear Spectroscopy in Strong Fields," Chem. Phys., Vol 75, 1983, pp 133-155.

4. Prior, Y., A.R. Bogdan, M.W. Dagenais and N. Bloembergen, "Pressure-Induced Extra Resonances in Four-Wave Mixing." Phys. Rev Lett., Vol. 46, 1981, pp. 111-114..

5. Dick, B., and R.M. Hochstrasser, "Fully Resonant Sum and Difference Frequency Mixing Spectroscopy," Ber. Bunsenges. Phys. Chem., Vol 89, 1985, pp. 344-346.

6. Verdieck, J.F., and P.A. Bonczyk, "Laser-Induced Saturated Fluorescence Investigations of CH, CN and NO in Flames," Proc. 18th Symp. (Int.) on Combust., 1981, pp. 1559-1566.

7. Dutta, P.K., R. Dallinger, and Thomas G. Spiro. "Resonance CARS Line Shapes via Frank-Condon Scattering," J. Chem. Phys., Vol. 73, 1980, pp. 3580-3585.

8. Carreira, L.A., L.P. Goss, and Thomas B. Malloy, Jr., " Experimental Evidence on the Source of Negative Peaks in CARS Spectra." J. Chem. Phys., Vol. 66, 1977, pp. 4360-4366.

9. Attal, B., D.Debarre, K. Muller-Dethlefs, and J-P. E. Taran, "Resonance-Enhanced CARS in C_2," Revue de Phys. Appl., Vol. 18, 1983, pp. 39-50.

10. Littman, Michael G., "Single-Mode Pulsed Tunable Dye Laser", Applied Optics, Vol. 23, 1984, pp. 4465-4468.

11. Littman, Michael G., Private Communication

12. Kumar, P., and R.S. Bondurant, "Improving the pulse shape in dye laser amplifiers: a new technique", Applied Optics, Vol 22, 1983, pp. 1284-1287.

13. Coxon, J.A., "Optimum molecular constants and term values for the X and A states of OH", Can. J. Phys., Vol. 58, 1980, pp. 993-949.

14. Dieke, G.H., and H.M. Crosswhite, "The ultraviolet bands of OH", J. Quant. Spectrosc. Radiat. Transfer, Vol. 2, 1962, pp. 97-199.

15. Cattolica, R.J., S. Yoon, and E.L. Knuth., "OH Concentration in an Atmospheric-Pressure Methane-Air Flame from Molecular-Beam Mass Spectrometry and Laser-Absorption spectroscopy," Sandia Laboratory Report SAND80-8804, 1980.

16. Anderson, William R., Leon J Decker, and Anthony J. Kotlar, "Temperature Profile of a Stoichiometric CH_4/N_2O Flame from Laser Excited Fluorescence Measurements on OH," Comb. and Flame, Vol. 48, 1982, pp. 163-176.

Acknowledgements

Discussions with Michael G. Littman of Princeton University concerning the design and operation of the single-mode dye laser are gratefully acknowledged. Suggestions of John H. Stufflebeam with regard to demodulators were very helpful. We thank Edward Dzwonkowski, Normand Gantick, and William Landry for their excellent technical assistance, and Ms Jan Sniffin for preparing figures.

FIG. 1

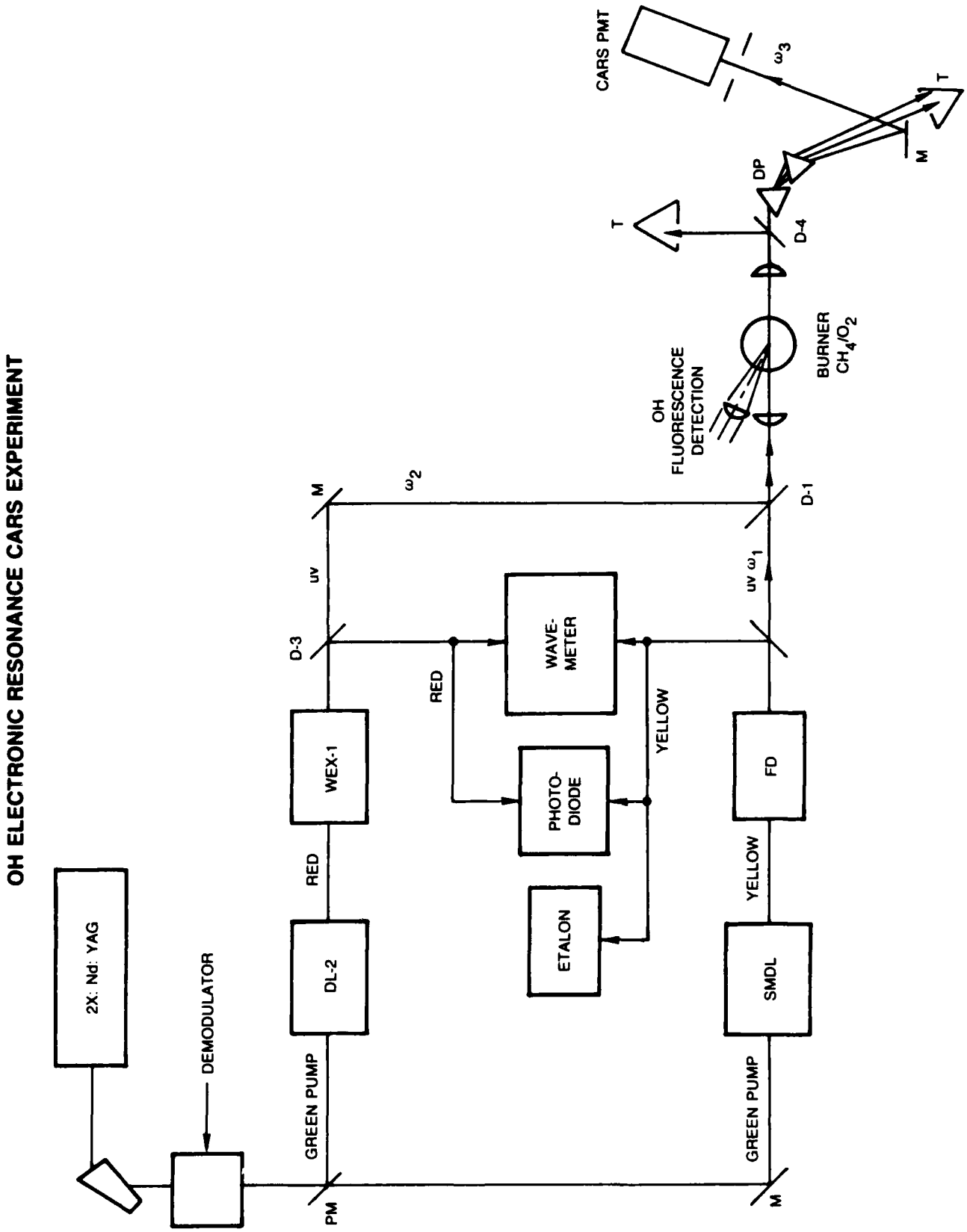
OH ELECTRONIC RESONANCE CARS EXPERIMENT
2X: Nd: YAG
DEMODULATOR
GREEN PUMP
PM
DL-2
RED
WEX-1
uv
D-3
M
ω_2
RED
WAVE-METER
PHOTO-DIODE
ETALON
YELLOW
uv ω_1
D-1
OH FLUORESCENCE DETECTION
BURNER CH_4/O_2
D-4
T
DP
M
T
ω_3
CARS PMT
GREEN PUMP
M
SMDL
YELLOW
FD

86-5-46-1

FIG. 2

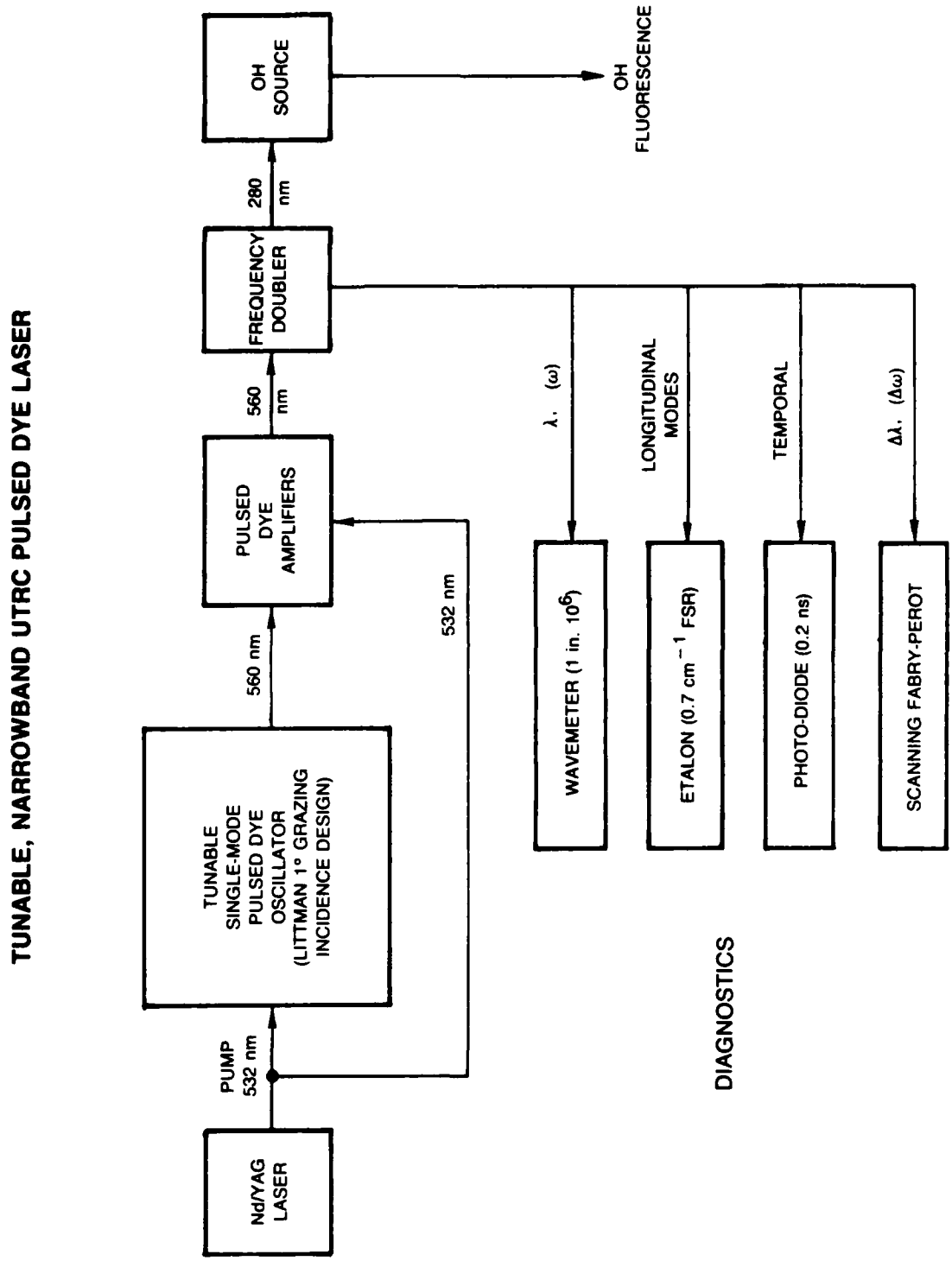
TUNABLE, NARROWBAND UTRC PULSED DYE LASER
Nd/YAG LASER
PUMP 532 nm
TUNABLE SINGLE-MODE PULSED DYE OSCILLATOR (LITTMAN 1° GRAZING INCIDENCE DESIGN)
560 nm
532 nm
PULSED DYE AMPLIFIERS
560 nm
FREQUENCY DOUBLER
280 nm
OH SOURCE
OH FLUORESCENCE
λ, (ω)
LONGITUDINAL MODES
TEMPORAL
Δλ, (Δω)
WAVEMETER (1 in. 10^6)
ETALON (0.7 cm^-1 FSR)
PHOTO-DIODE (0.2 ns)
SCANNING FABRY-PEROT
DIAGNOSTICS

86-5-46-2

Figure 3

Photograph of pulsed oscillator for UTRC tunable single mode dye laser (SMDL). Oscillator is based on single-mode Littman 1° grazing incidence grating design with tuning mirror mounted on rotation stage.

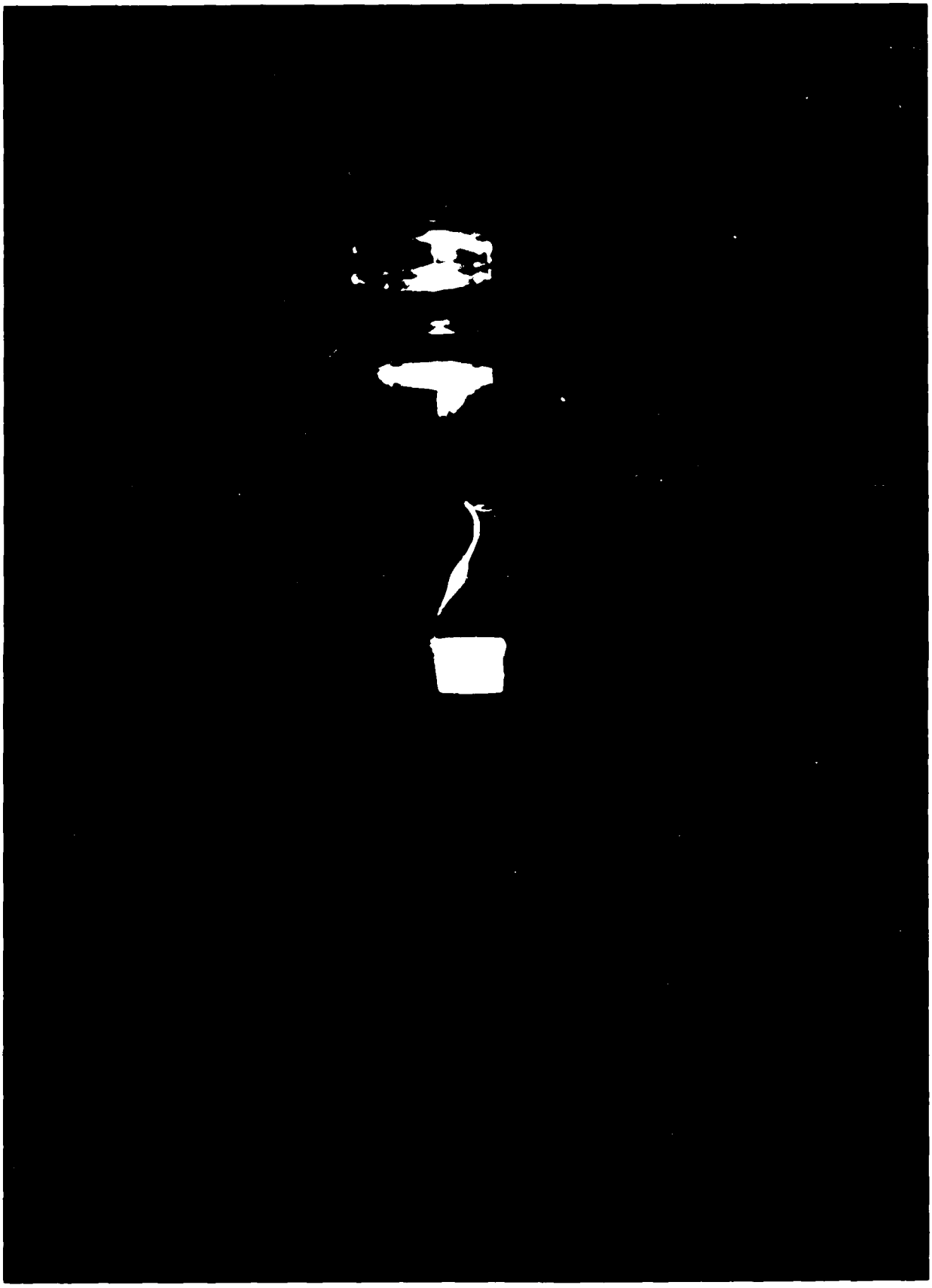

FIG. 4

Projected ring patterns through 0.7 cm^{-1} FSR etalon for single mode dye laser amplified beam (SMDL) tuned near 560 nm.

a) Single longitudinal mode pattern

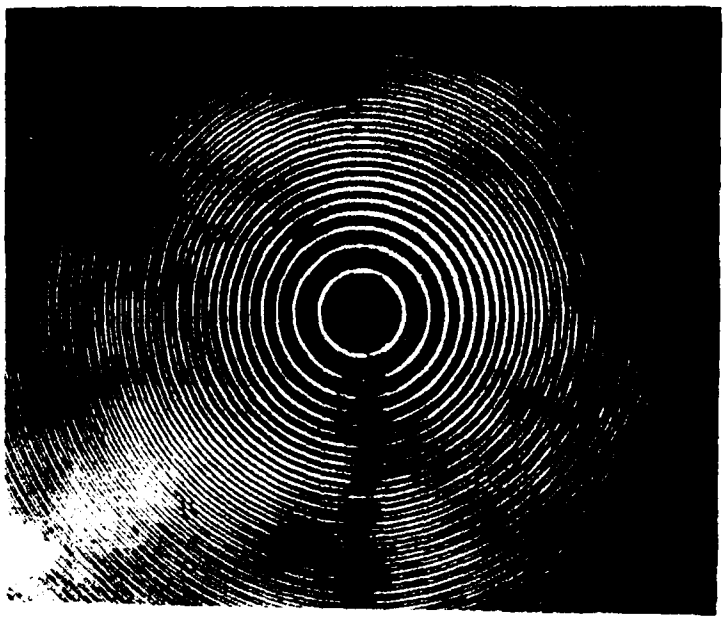

b) Dominant single-mode with weak adjacent longitudinal modes (weak rings near center intense ring)

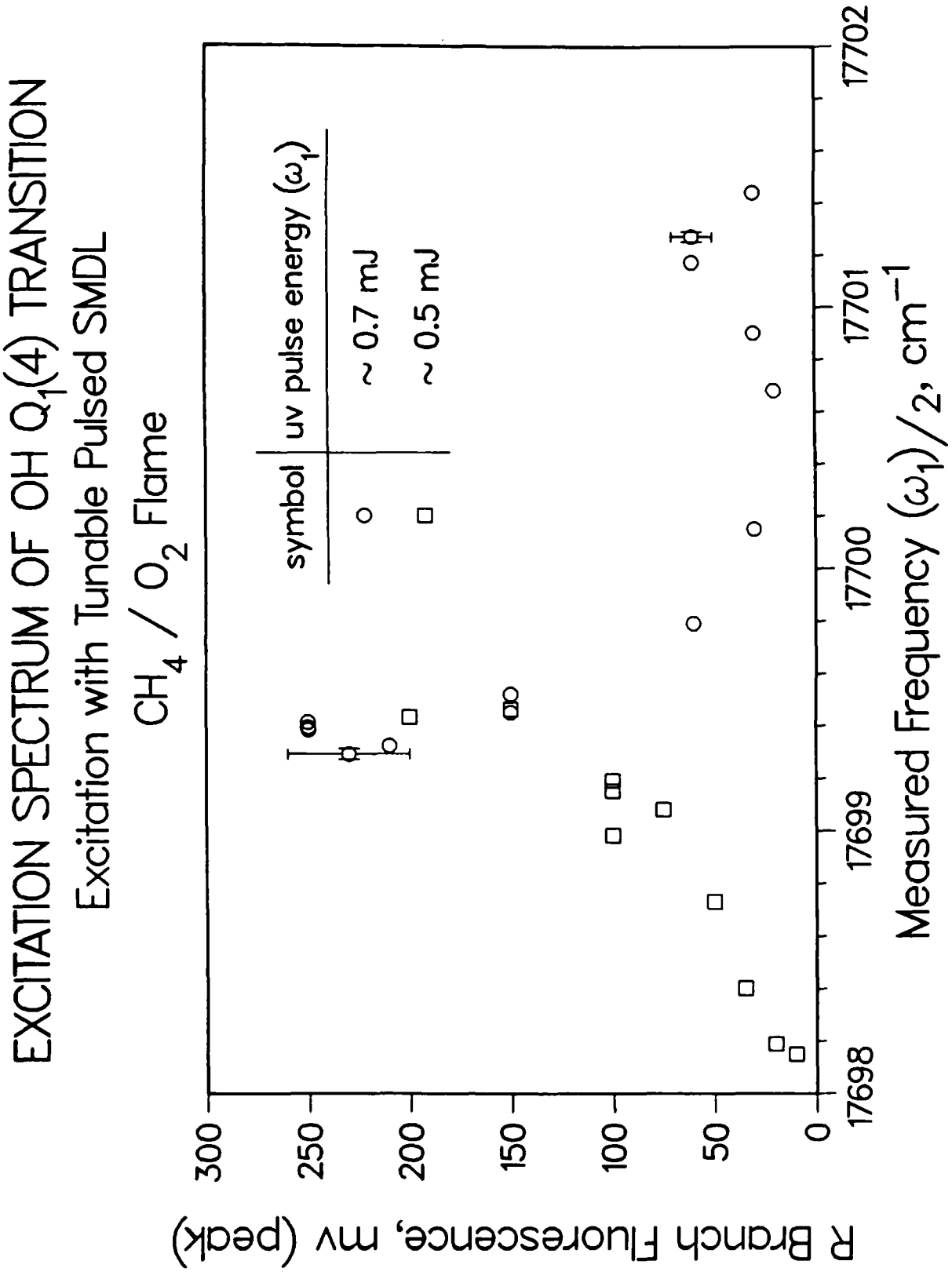
EXCITATION SPECTRUM OF OH $Q_1(4)$ TRANSITION
Excitation with Tunable Pulsed SMDL
CH_4 / O_2 Flame
symbol
uv pulse energy (ω_1)
~ 0.7 mJ
~ 0.5 mJ
R Branch Fluorescence, mv (peak)
300
250
200
150
100
50
0
17698
17699
17700
17701
17702
Measured Frequency $(\omega_1)/2$, cm^{-1}

FIG. 6

Temporal behavior of pump and Stokes beam pulses for OH electronic resonance CARS experiment. Photos show two sequential pulses.

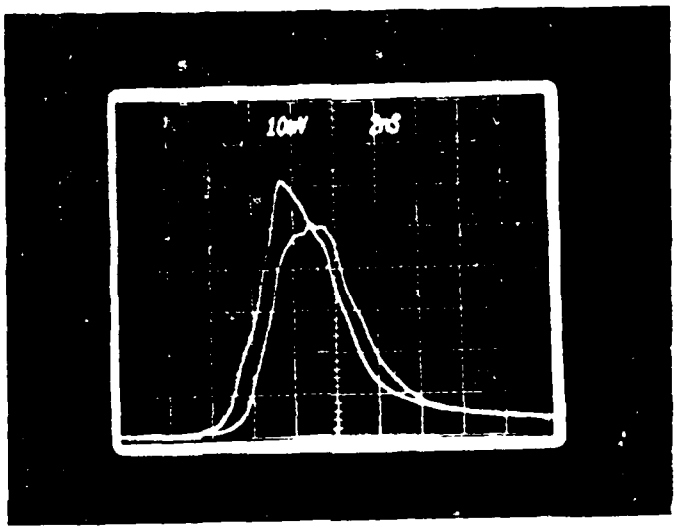

a) CARS pump beam at $\omega_1/2$

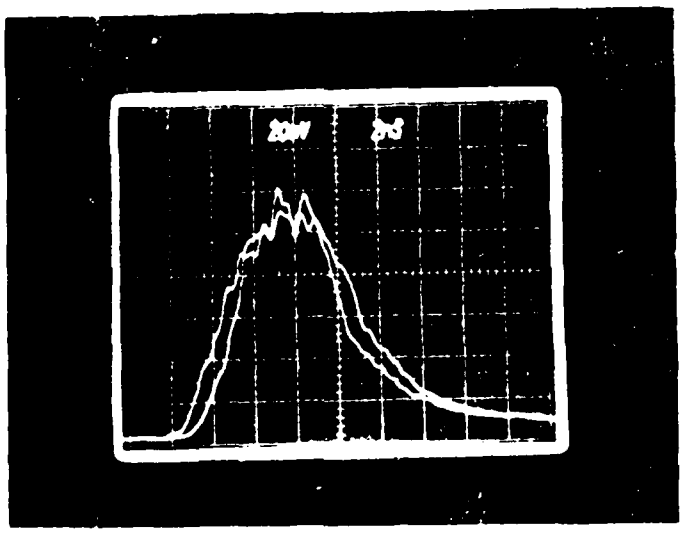

b) CARS Stokes beam at $\omega_2/2$

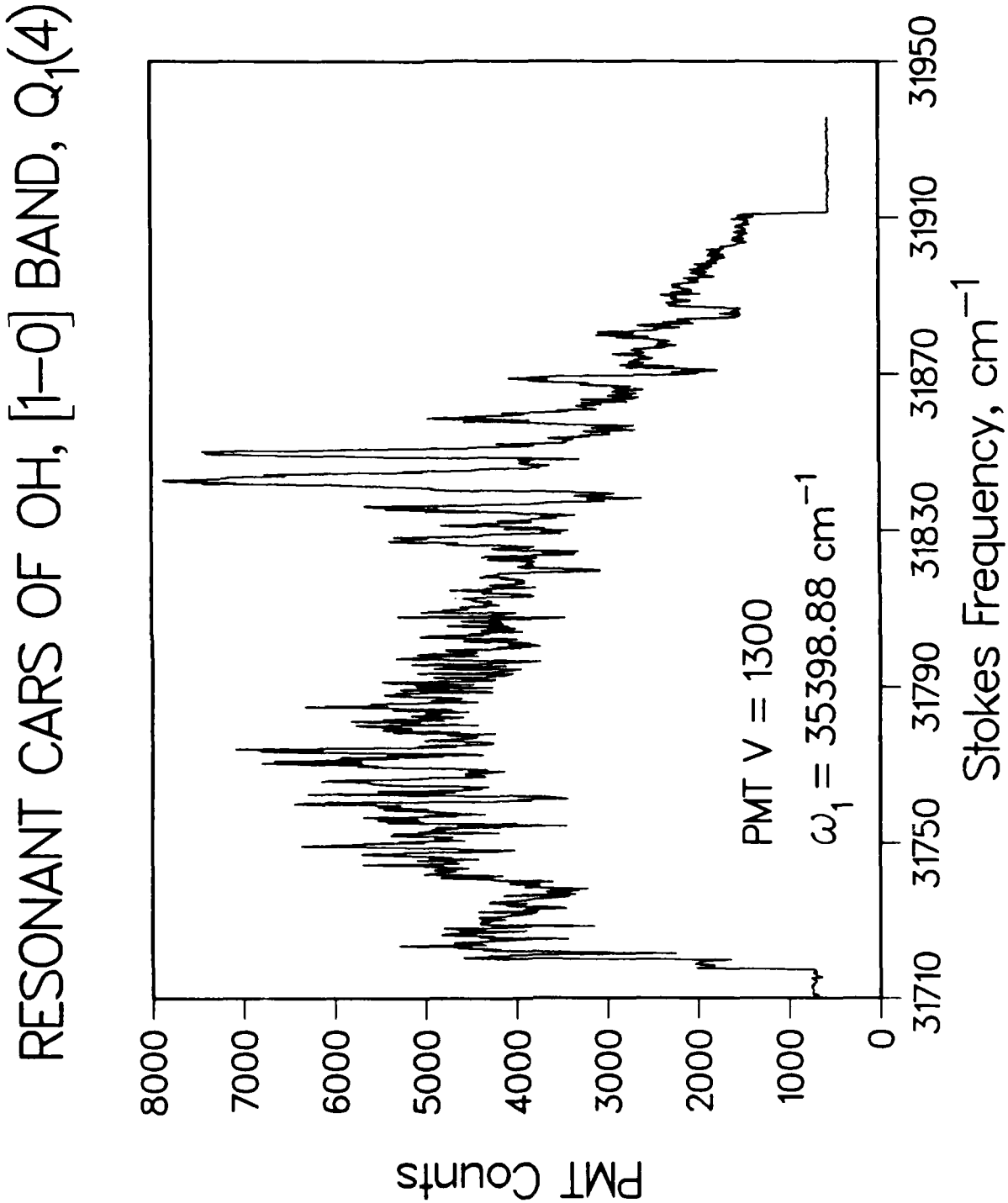
RESONANT CARS OF OH, [1–0] BAND, $Q_1(4)$
PMT Counts
8000
7000
6000
5000
4000
3000
2000
1000
0
31710
31750
31790
31830
31870
31910
31950
Stokes Frequency, cm^{-1}
PMT V = 1300
ω_1 = 35398.88 cm^{-1}

FIG. 8

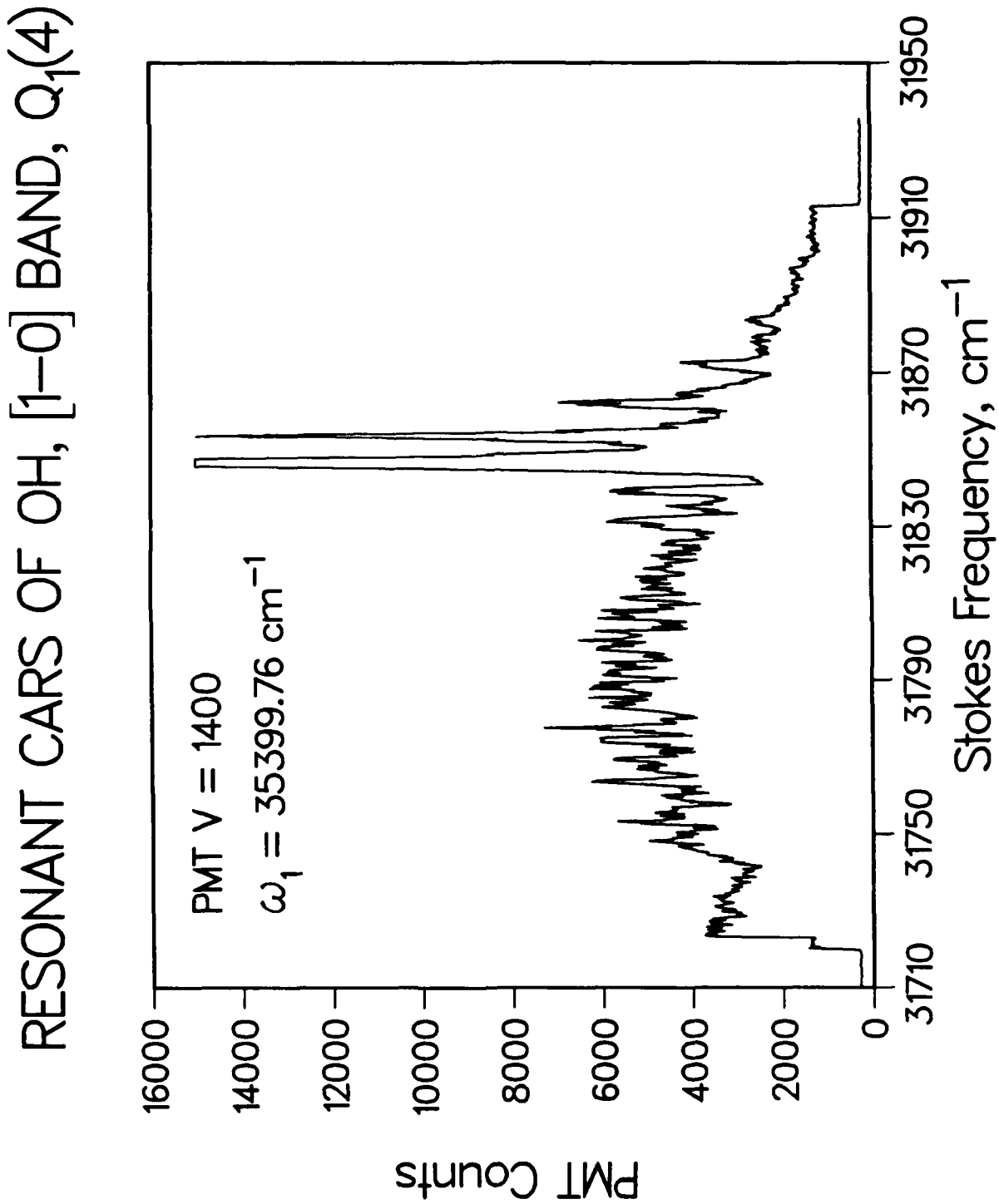
RESONANT CARS OF OH, [1–0] BAND, $Q_1(4)$
PMT V = 1400
ω_1 = 35399.76 cm^{-1}
PMT Counts
16000
14000
12000
10000
8000
6000
4000
2000
0
31710
31750
31790
31830
31870
31910
31950
Stokes Frequency, cm^{-1}

FIG. 9

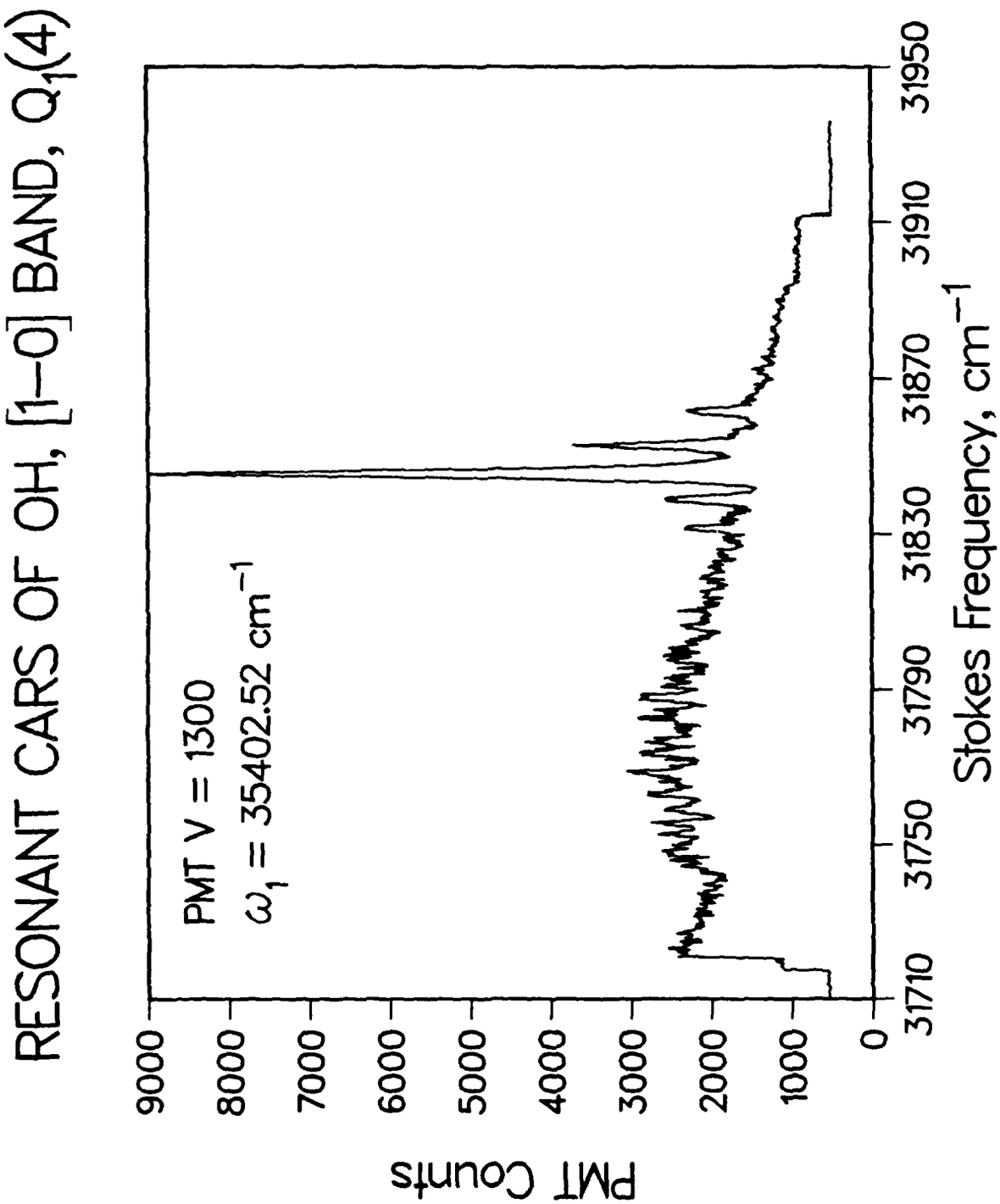
RESONANT CARS OF OH, [1–0] BAND, $Q_1(4)$
PMT V = 1300
ω_1 = 35402.52 cm^{-1}
PMT Counts
9000
8000
7000
6000
5000
4000
3000
2000
1000
0
31710
31750
31790
31830
31870
31910
31950
Stokes Frequency, cm^{-1}

FIG. 10

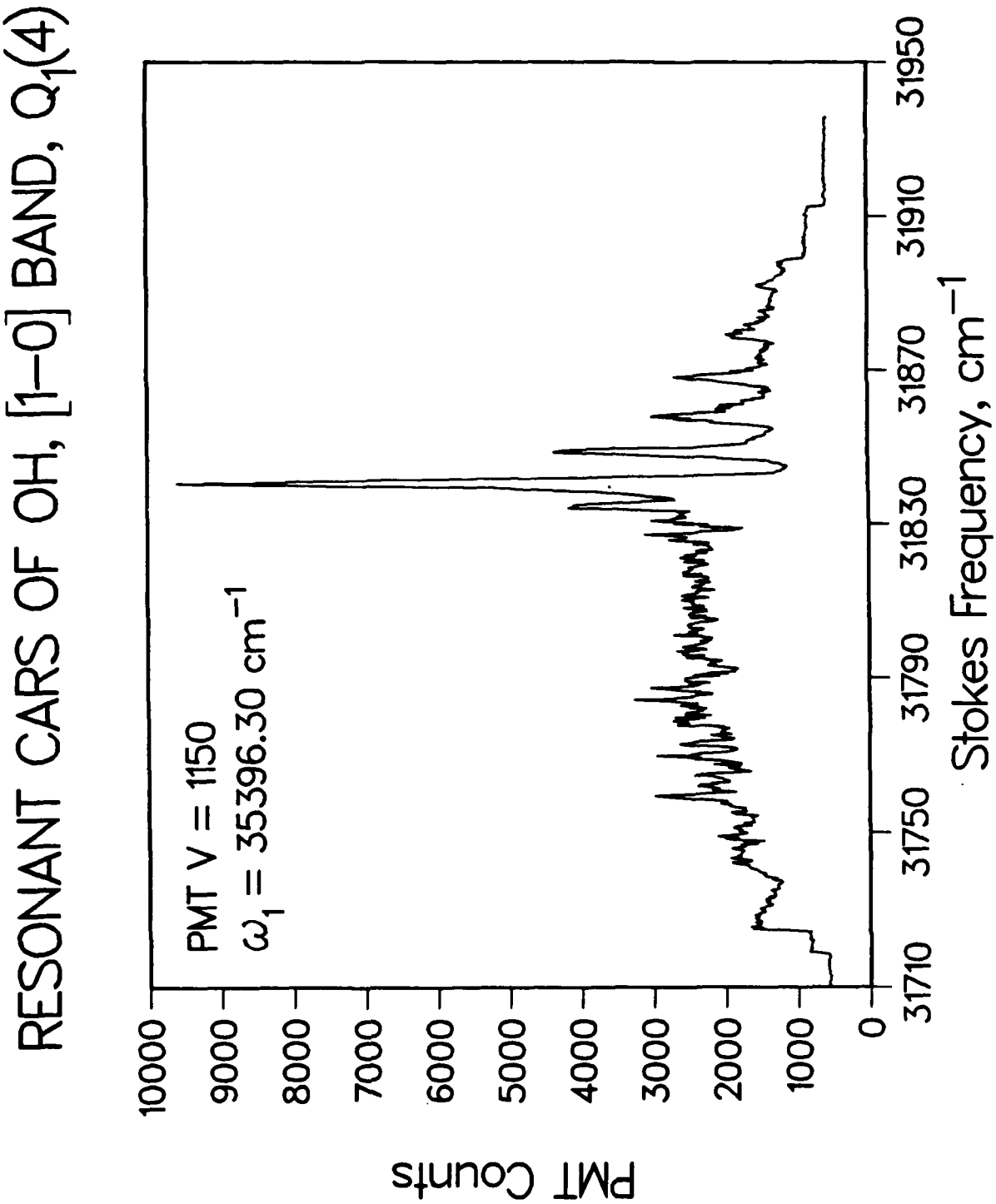
RESONANT CARS OF OH, [1–0] BAND, $Q_1(4)$
PMT V = 1150
ω_1 = 35396.30 cm^{-1}
PMT Counts
10000
9000
8000
7000
6000
5000
4000
3000
2000
1000
0
31710
31750
31790
31830
31870
31910
31950
Stokes Frequency, cm^{-1}

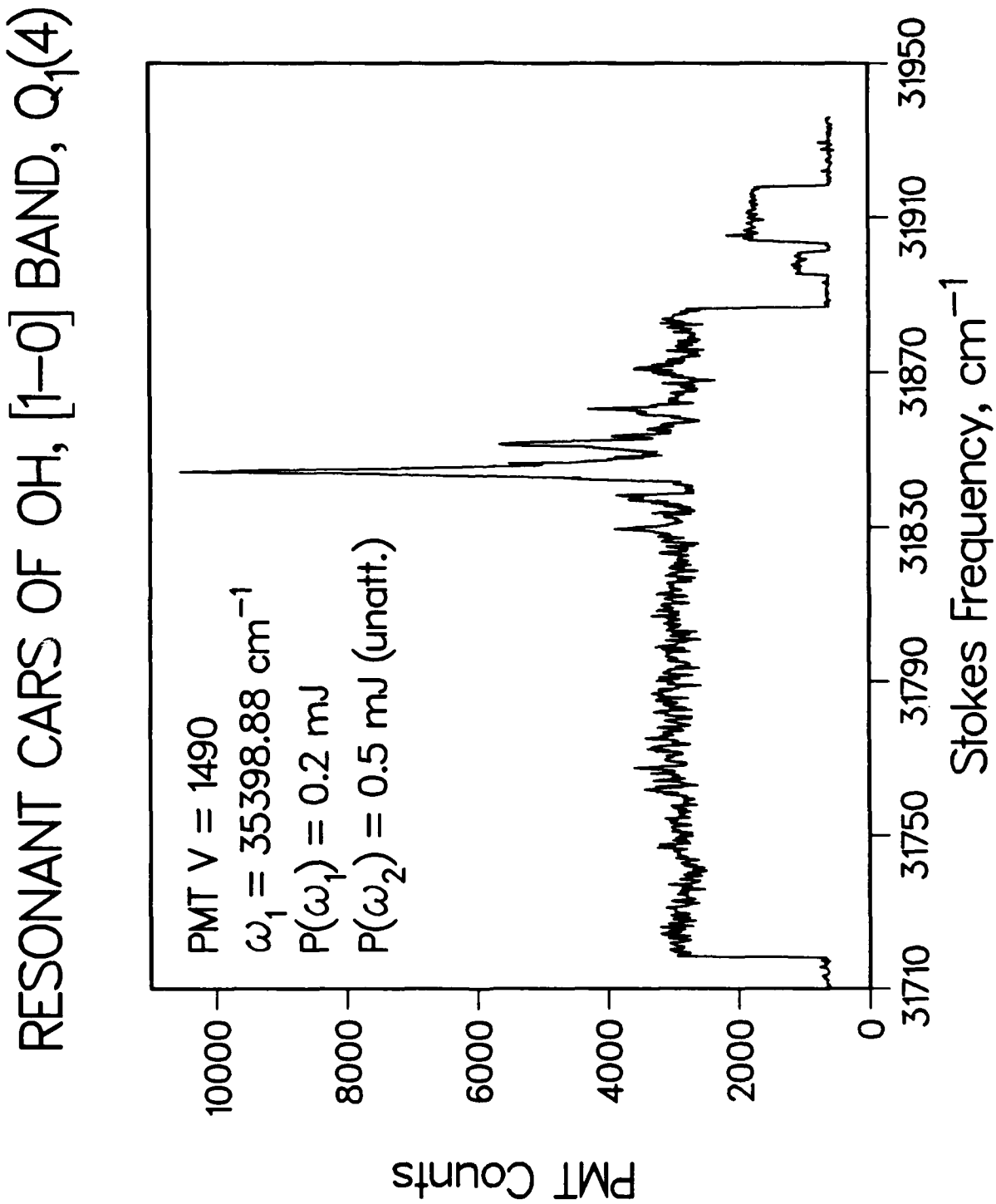
RESONANT CARS OF OH, [1–0] BAND, $Q_1(4)$
PMT V = 1490
ω_1 = 35398.88 cm^{-1}
$P(\omega_1)$ = 0.2 mJ
$P(\omega_2)$ = 0.5 mJ (unatt.)
PMT Counts
10000
8000
6000
4000
2000
0
31710
31750
31790
31830
31870
31910
31950
Stokes Frequency, cm^{-1}

FIG. 12

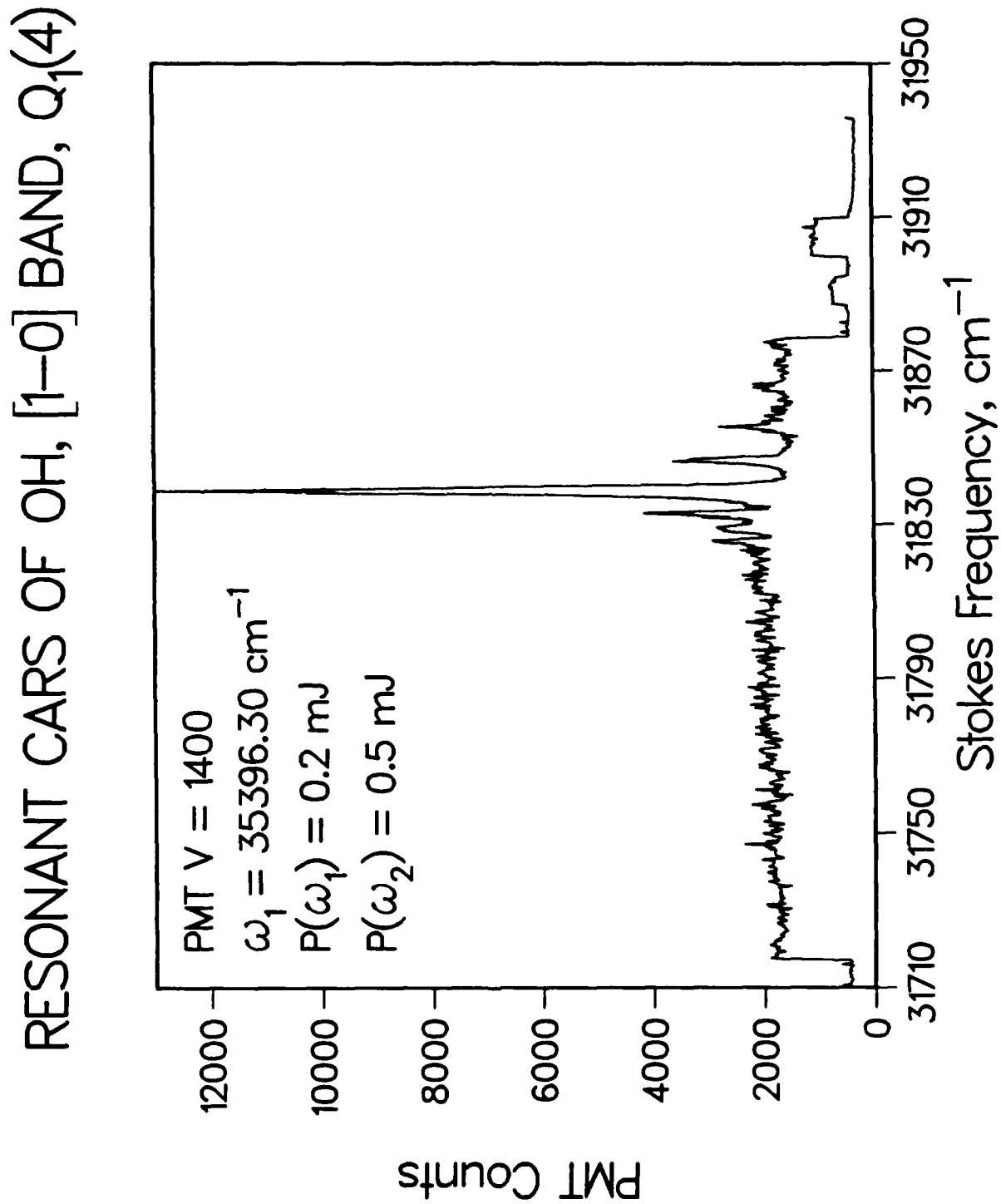
RESONANT CARS OF OH, [1–0] BAND, $Q_1(4)$
PMT V = 1400
ω_1 = 35396.30 cm^{-1}
$P(\omega_1)$ = 0.2 mJ
$P(\omega_2)$ = 0.5 mJ
PMT Counts
12000
10000
8000
6000
4000
2000
0
31710
31750
31790
31830
31870
31910
31950
Stokes Frequency, cm^{-1}

FIG. 13

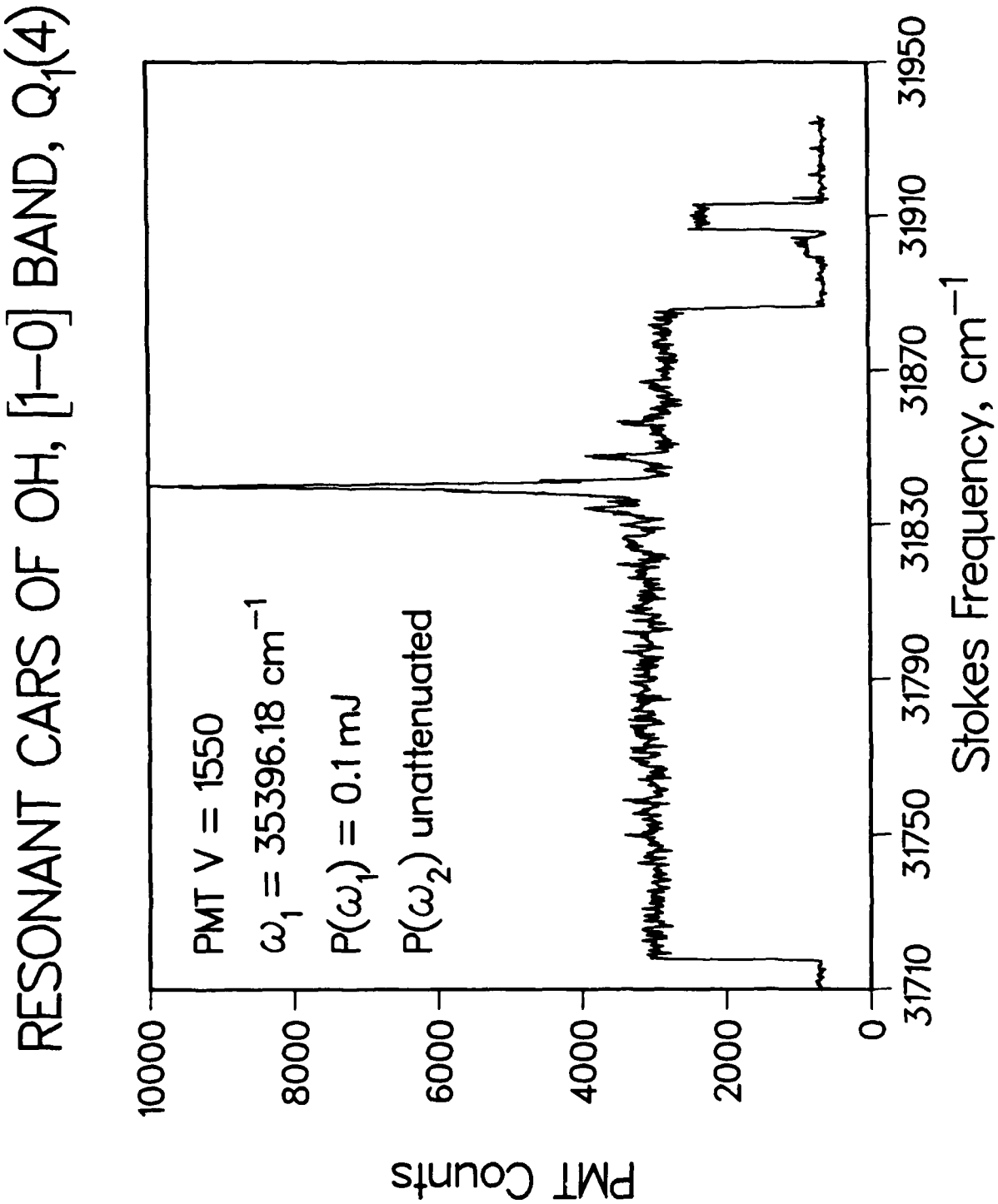
RESONANT CARS OF OH, [1–0] BAND, $Q_1(4)$
PMT V = 1550
ω_1 = 35396.18 cm^{-1}
$P(\omega_1)$ = 0.1 mJ
$P(\omega_2)$ unattenuated
PMT Counts
10000
8000
6000
4000
2000
0
31710
31750
31790
31830
31870
31910
31950
Stokes Frequency, cm^{-1}

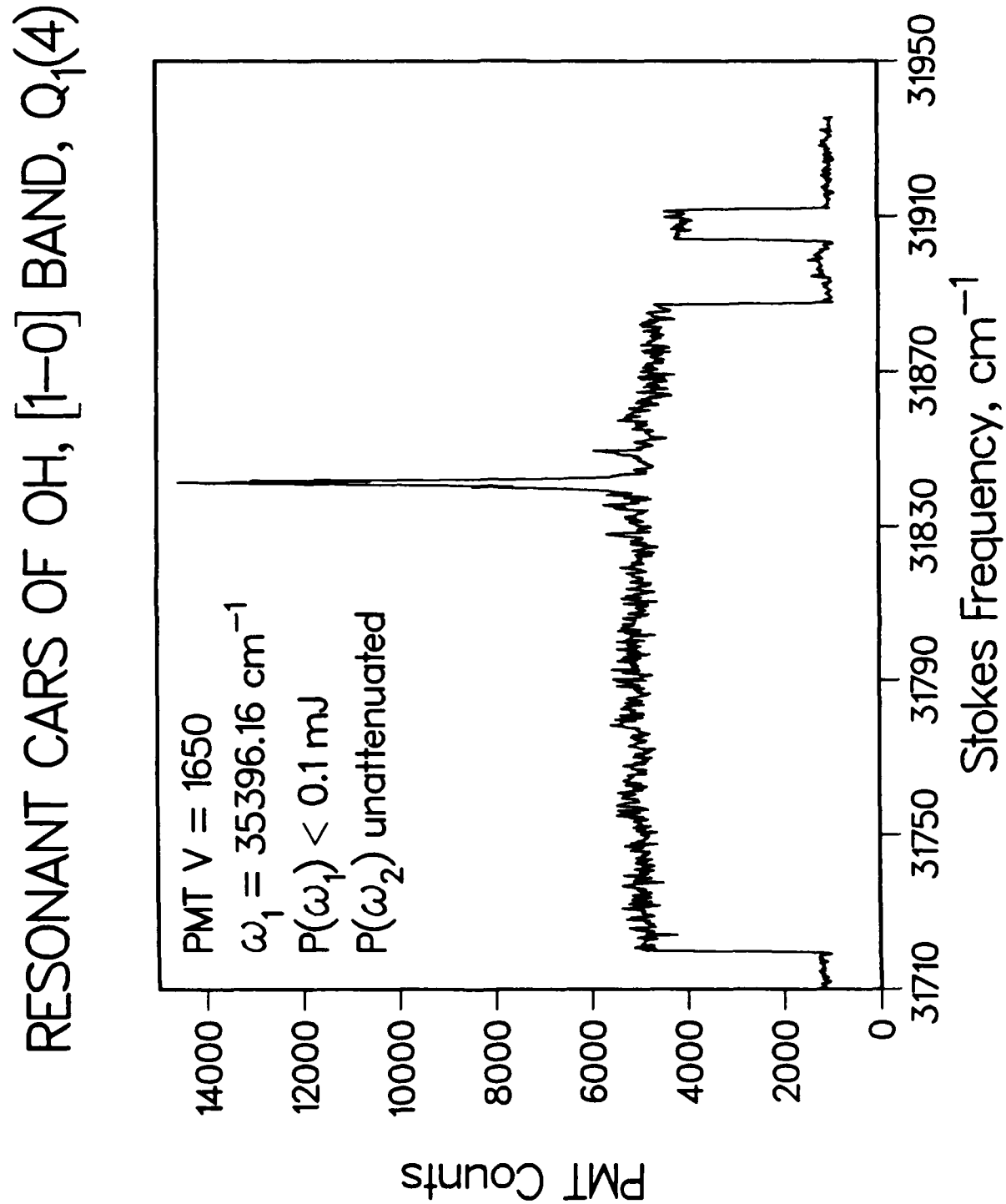
RESONANT CARS OF OH, [1–0] BAND, $Q_1(4)$
PMT V = 1650
ω_1 = 35396.16 cm^{-1}
$P(\omega_1) < 0.1$ mJ
$P(\omega_2)$ unattenuated
PMT Counts
0
2000
4000
6000
8000
10000
12000
14000
31710
31750
31790
31830
31870
31910
31950
Stokes Frequency, cm^{-1}

FIG. 15

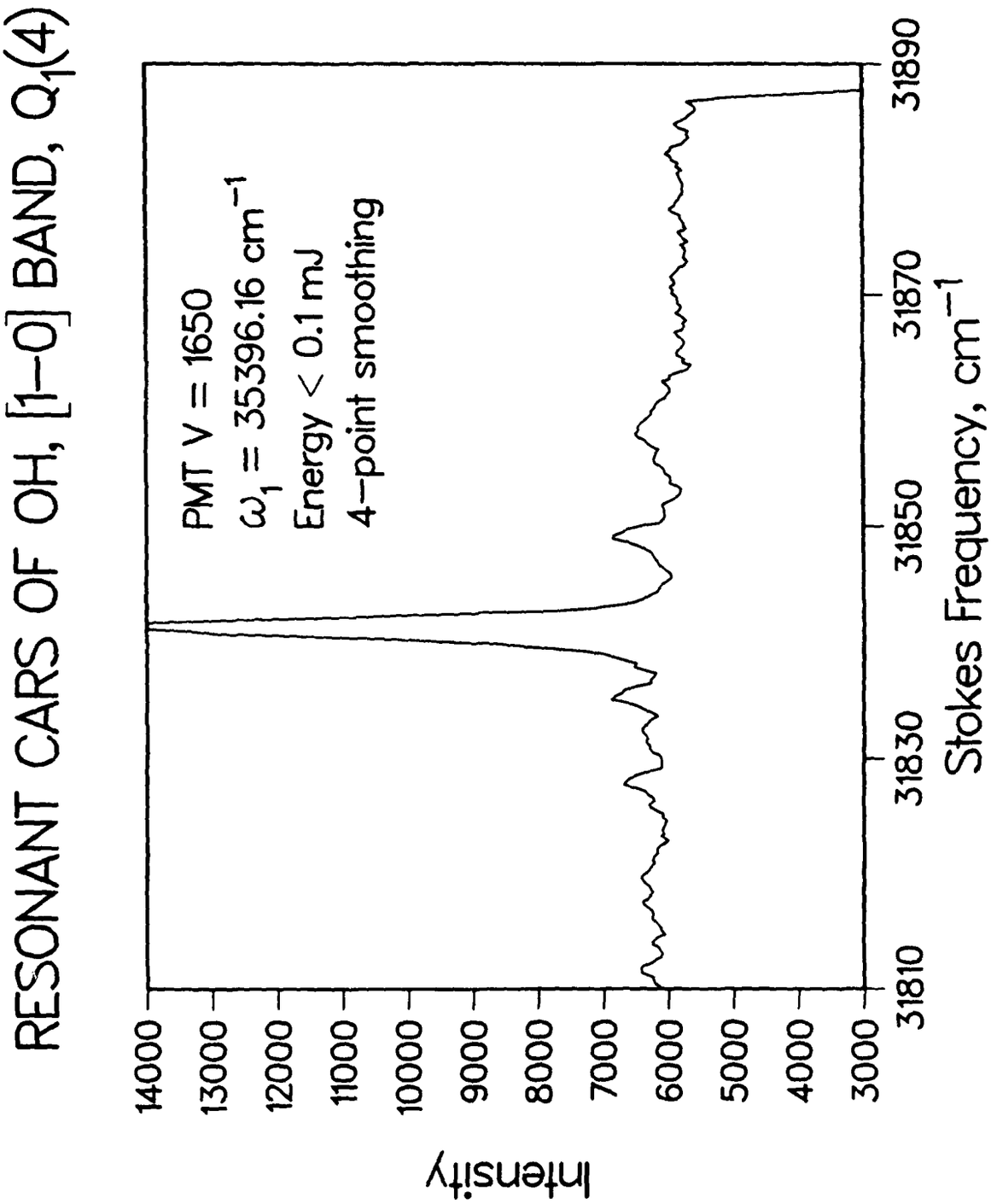
RESONANT CARS OF OH, [1–0] BAND, $Q_1(4)$
PMT V = 1650
ω_1 = 35396.16 cm^{-1}
Energy < 0.1 mJ
4–point smoothing
Intensity
14000
13000
12000
11000
10000
9000
8000
7000
6000
5000
4000
3000
31810
31830
31850
31870
31890
Stokes Frequency, cm^{-1}

FIG. 16

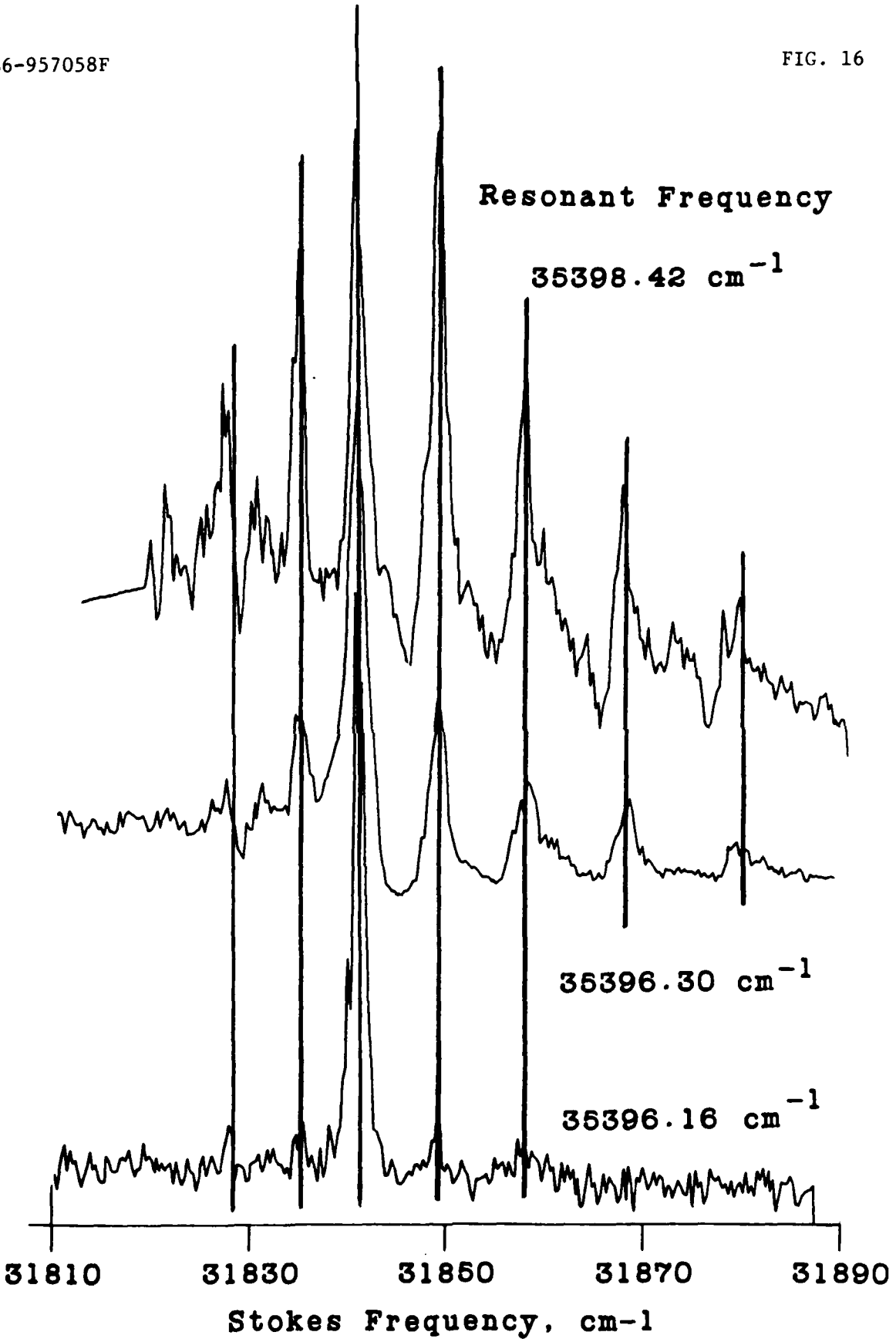

Constancy of Line Splittings

END

1-87

DTIC